Applied Radiation and Isotopes 206 (2024) 111220

Contents lists available at ScienceDirect

Applied Radiation and Isotopes

journal homepage: www.elsevier.com/locate/apradiso

^{44}Sc production from enriched $^{47}TiO_2$ targets with a medical cyclotron

Gaia Dellepiane [a,*,1], Pierluigi Casolaro [a,2], Alexander Gottstein [a], Isidre Mateu [a], Paola Scampoli [a,b], Saverio Braccini [a]

[a] Albert Einstein Center for Fundamental Physics (AEC), Laboratory for High Energy Physics (LHEP), University of Bern, Sidlerstrasse 5, CH-3012 Bern, Switzerland

[b] Department of Physics "Ettore Pancini", University of Napoli Federico II, Complesso Universitario di Monte S. Angelo, 80126 Napoli, Italy

ARTICLE INFO

Keywords:
Scandium-44
PET imaging
Theranostics
Cross sections
Proton irradiation
Medical cyclotron
Solid targets

ABSTRACT

^{44}Sc is a β^+-emitter which has been extensively studied for nuclear medicine applications. Its promising decay characteristics [$t_{1/2}$ = 3.97 h, E_{β^+} = 632 keV (94.3%), E_γ = 1157 keV (99.9%); 1499 keV (0.91%)] make it highly attractive for clinical PET imaging, offering an alternative to the widely used ^{68}Ga [$t_{1/2}$ = 67.7 min, E_{β^+} = 836 keV (87.7%)]. Notably, its nearly fourfold longer half-life opens avenues for applications with biomolecules having extended biological half-lives and enables the centralized distribution of ^{44}Sc radiopharmaceuticals. An additional advantage of employing ^{44}Sc as a diagnostic radioisotope lies in its counterpart, the β^--emitter ^{47}Sc, which is currently under investigation for targeted radiotherapy. Together, they form an ideal theranostic pair, providing a comprehensive solution for both diagnostic imaging and therapeutic applications in nuclear medicine.

At the Bern medical cyclotron, a study to optimize the production of scandium radioisotopes is currently ongoing. In this context, proton irradiation of titanium targets has been investigated, exploiting the reactions ^{47}Ti(p,α)^{44}Sc and ^{50}Ti(p,α)^{47}Sc. This approach enables the production of Sc radioisotopes within a single PET medical cyclotron facility, employing identical chemical procedures for target preparation and post-irradiation processing.

In this paper, we report on cross-section measurements of the ^{47}Ti(p,α)^{44}Sc nuclear reaction using 95.7% enriched $^{47}TiO_2$ targets. On the basis of the obtained results, the production yield and purity were calculated to assess the optimal irradiation conditions. Production tests were performed to confirm these findings.

1. Introduction

The future of nuclear medicine relies on the availability of novel radionuclides with suitable physical and chemical characteristics, in quantities and qualities appropriate for clinical applications. The theranostic approach aims at personalizing the medical treatments on the basis of each patient's specific characteristics, by labeling the same molecule of biomedical interest with a pair of radionuclides, one for diagnosis (β^+- or γ- emitter) and one for therapy (β^--, α-, or Auger electron emitter). For this to be possible, the two radionuclides must undergo the same metabolic processes within the body, ideally belonging to the same chemical element. In this context, scandium is garnering significant attention as it provides two true theranostic pairs, namely ^{43}Sc/^{47}Sc and ^{44}Sc/^{47}Sc.

^{44}Sc [$t_{1/2}$ = 4.042 h (Durán et al., 2022), E_{β^+} = 632 keV (94.3%), E_γ = 1157 keV (99.9%); 1499 keV (0.91%)] is a β^+-emitter with interesting decay properties for PET imaging and it was proposed as an alternative to ^{68}Ga for pre-therapeutic imaging and monitoring the response to radionuclide therapy (van der Meulen et al., 2015). Its half-life of about 4 h makes it suitable to label molecules with a relatively long biological half-life, covering several hours after the administration of the radioactive compounds (Müller et al., 2013). Furthermore, it would allow for centralized production and cost-efficient distribution of ^{44}Sc-labeled radiopharmaceuticals to distant PET centers.

Many ^{44}Sc production routes are reported in the literature, as shown in Table 1. Among them, the use of enriched ^{44}CaO targets was investigated at the Bern medical cyclotron in collaboration with the Paul Scherrer Institute (PSI), resulting in a ^{44}Sc production yield of 15 GBq (van der Meulen et al., 2020). This study demonstrated that the use of CaO targets presents fewer radioprotection concerns compared to the widely reported $CaCO_3$ targets (van der Meulen et al., 2015;

* Corresponding author.
E-mail addresses: gaia.dellepiane@unibe.ch, gaia.dellepiane@lhep.unibe.ch (G. Dellepiane).
[1] Now at Paul Scherrer Institute, 5232 Villigen, Switzerland.
[2] Now at Department of Physics "Ettore Pancini", University of Napoli Federico II, Complesso Universitario di Monte S. Angelo, 80126 Napoli, Italy.

https://doi.org/10.1016/j.apradiso.2024.111220
Received 1 December 2023; Received in revised form 18 January 2024; Accepted 28 January 2024
Available online 29 January 2024

Table 1
Main ^{44}Sc production routes reported in the literature.

Impinging particle	Target	Route
p	^{44}Ca	^{44}Ca(p,n)^{44}Sc (van der Meulen et al., 2015, 2020; Sitarz et al., 2018; Carzaniga et al., 2017; Krajewski et al., 2013)
	^{47}Ti	^{47}Ti(p,α)^{44}Sc (Loveless et al., 2021; Levkowskij, 1991)
	^{45}Sc	^{45}Sc(p,2n)^{44}Ti → ^{44}Sc (Roesch, 2012; Radchenko et al., 2016)
d	^{44}Ca	^{44}Ca(d,2n)^{44}Sc (Sitarz et al., 2018)
α	^{42}Ca	^{42}Ca(α,d)^{44}Sc (Szkliniarz et al., 2016)

Sitarz et al., 2018). However, the handling of these targets still requires special care due to the high hygroscopicity of CaO, necessitating the target to be prepared and stored under Ar atmosphere and to be irradiated as soon as possible to prevent it from swelling. Furthermore, the low isotopic abundance of ^{44}Ca (2.09% (CIAAW, 2023)) can render this production method costly and constrained by limited supply.

In the framework of a research program ongoing at the Bern medical cyclotron laboratory aimed at the production of Sc radioisotopes through proton irradiation of Ti targets (Carzaniga et al., 2017; Dellepiane et al., 2022c), the ^{47}Ti(p,α)^{44}Sc nuclear reaction was investigated. The use of titanium could enable the production of Sc radioisotopes in a single PET medical cyclotron facility, using a unified separation methodology that makes use of identical targetry and target-processing chemistries (Loveless et al., 2021).

To maximize the ^{44}Sc activity, while minimizing the production of other Sc radioimpurities, the precise knowledge of the nuclear cross sections as a function of the beam energy is of paramount importance. Data reported in the literature and accessible via the EXFOR database (https://www-nds.iaea.org/exfor/) are scarce and do not fully cover the energy range of a medical cyclotron (up to 25 MeV (Braccini, 2017)).

In this paper we report on the cross-section measurement of the nuclear reaction ^{47}Ti(p,α)^{44}Sc, obtained irradiating 95.7% enriched $^{47}TiO_2$ targets. The cross section of the nuclear reactions producing other Sc radioisotopes in the energy range of interest, namely ^{47}Ti(p,αn)^{43}Sc, ^{47}Ti(p,α)^{44m}Sc, ^{47}Ti(p,2p)^{46}Sc and ^{48}Ti(p,2p)^{47}Sc, are also presented.

The results obtained were used to assess the optimal irradiation conditions to maximize the production yield and the radionuclidic purity. Production tests were performed to confirm these calculations based on cross-section measurements.

2. Materials and methods

2.1. The Bern medical cyclotron laboratory

The cyclotron laboratory at the Bern University Hospital (Inselspital) (Braccini, 2013) is based on a IBA Cyclone 18/18 high current cyclotron (18 MeV proton beams, beam currents from a few pA to 150 μA (Auger et al., 2015), 8 exit ports). It is housed in its own bunker, while a second bunker, with independent access, is available for research activities. This configuration is unusual for a hospital-based facility and allows to perform both ^{18}F-labeled PET tracer production and multidisciplinary research activities (Braccini and Scampoli, 2016). For the latter purpose, a 6-m-long Beam Transport Line (BTL) is installed at the Bern medical cyclotron, delivering the beam to the second bunker. The BTL is characterized by an extracted beam energy of (18.3 ± 0.4) MeV (Nesteruk et al., 2018; Häffner et al., 2019) and it is equipped with beam focusing and diagnostic systems, including a non-destructive two-dimensional beam profiler based on scintillating doped silica fibers passing through the beam. The detector, named UniBEaM, was developed by our group and commercialized by the company D-Pace (Auger et al., 2016; Potkins et al., 2017).

The production of ^{44}Sc was studied by irradiating a 95.7% enriched $^{47}TiO_2$ powder purchased by Isoflex (Isoflex, 2022). The isotopic composition of the material is reported in Table 2.

Table 2
Isotopic abundance in enriched ^{47}Ti oxide supplied by Isoflex (Isoflex, 2022).

	^{46}Ti	^{47}Ti	^{48}Ti	^{49}Ti	^{50}Ti
47-enr. [%]	0.41	95.7	3.57	0.18	0.14

The produced activities were assessed with an N-type high purity germanium (HPGe) detector (Canberra2019), coupled to a preamplifier and to a Lynx® digital signal analyzer. The energy spectrum of the source was acquired with the Genie2k (Mirion Technologies, 2022) software in the case of a single measurement and with the Excel2Genie (Forgács et al., 2014) Microsoft Excel application for repeated measurements. The analysis was carried out with the InterSpec software (Sandia National Laboratories, 2022), developed by the Sandia National Laboratories. The efficiency calibration was performed in accordance with the international standard (International Standard, 2021) by means of a multi-peak γ source (^{57}Co, ^{60}Co, ^{85}Sr, ^{88}Y, ^{109}Cd, ^{133}Sn, ^{137}Cs and ^{241}Am). The source had the same size and shape of the targets and it was measured at distances up to 10 cm from the detector, using a custom-designed plexiglass ladder with equally spaced levels 1 cm apart. The calibration was tested in metrological studies (Durán et al., 2022), resulting in efficiency uncertainties below 3% (Juget et al., 2023).

The γ-lines used to identify the radionuclides of interest are listed in Table 3.

2.2. Material and procedure for cross-section measurements

Cross-section measurements were performed irradiating targets prepared with the sedimentation method. About 15 mg of TiO_2 powder were suspended in distilled water and deposited in a 4.2-mm-diameter, 0.8-mm-deep pocket in an aluminum disc. Once the water had completely evaporated by means of a heating plate, the deposited mass was measured with an analytical scale (Mettler Toledo XS204 DeltaRange), resulting in a mass uncertainty within 5%. The pocket was then sealed with a 13-μm thick aluminum foil to prevent material leakage throughout the irradiation and measurement procedure. With this method, targets with an average thickness of 15 μm can be achieved, and consequently the energy remains constant within the uncertainty over the full irradiated mass.

Each target was then irradiated with a proton beam with a flat spatial distribution, so that any inhomogeneity in thickness due to sedimentation does not play any role. This procedure, successfully used in our previous works on cross-section measurements (Dellepiane et al., 2022a,d,b, 2023), is described in detail in Ref. Carzaniga et al. (2017)

The beam was flattened by the optical elements of the BTL and monitored online with the UniBEaM detector. A specific target station, providing a beam of controlled diameter by means of a 8-mm-diameter collimator, was connected to an electrometer (B2985 A Keysight) for measuring the beam current on the target. An electron suppressor ring connected to a negative bias voltage (−50 V) is embedded in the station to repel secondary electrons produced during the irradiation, to prevent current overestimation. To obtain different impinging proton energies, the beam was degraded by means of aluminum attenuator discs placed in front of the target. The beam energy was then determined using the SRIM-2013 Monte Carlo code (Ziegler and Manoyan, 2013).

Table 3
Decay properties and main γ emissions of scandium radioisotopes. The values in parentheses are the uncertainties referred to the last digits of the value (IAEA, 2022).

Radioisotope	$t_{1/2}$	Decay mode: [%]	E_γ [keV]	BR [%]
^{43}Sc	3.891*(12)* h	ec + β^+: 100	372.9*(3)*	22.5*(7)*
^{44}Sc	4.042*(3)* h (Durán et al., 2022)	ec + β^+: 100	1499.46*(2)*	0.908*(15)*
^{44m}Sc	58.61*(10)* h	IT: 98.8	271.240*(10)*	86.75*(6)*
^{46}Sc	83.79*(4)* d	β^-: 100	889.277*(3)*	99.984*(1)*
^{47}Sc	3.3492*(6)* d	β^-: 100	159.381*(15)*	68.3*(4)*

The average irradiation time in each run was 13 min and the beam current about 6 nA. After the End of Beam (EoB), the produced activity was measured by γ spectrometry with the HPGe detector. In all measurements, the count frequency was sufficiently low to limit pile-up effects (dead time below 2%).

The main experimental uncertainty affecting the cross-section measurements was due to the flatness of the beam (5%). Other sources of uncertainties are the beam current integration (1%), the HPGe detector efficiency (3%) and the target mass measurements (4%). All the contributions were summed in quadrature.

2.3. Study of ^{44}Sc production yield and purity

Aiming at an optimized production of ^{44}Sc, a study of the Thick Target Yield (TTY) and of its purity was performed. The TTY as a function of the proton energy on target E can be calculated from the cross-section measurements using the following formula

$$TTY(E,t_i) = \frac{A(t_{EoB})}{I} = (1 - e^{-\lambda \cdot t_i}) \cdot \frac{N_A \cdot \eta}{m_{mol} \cdot q} \int_{E_{th}}^{E} \frac{\sigma(E')}{S_p(E')} dE' \quad (1)$$

where t_i is the irradiation time, I the current on target, $A(t_{EoB})$ the activity produced at EoB, λ the decay constant, $\sigma(E')$ the cross section as a function of the proton kinetic energy E', $S_p(E')$ is the mass stopping power for the target material, E_{th} is the threshold energy of the considered reaction, N_A the Avogadro constant, m_{mol} the average molar mass of the target material, η the number of target atoms of the desired species per molecule and q the charge of the projectile. The mass stopping power was calculated using SRIM.

If a thin target is used, so that the protons are not stopped therein, the production yield Y(E) can be defined as

$$Y(E) = TTY(E) - TTY(E_{out}) \quad (2)$$

where E_{out} is the proton energy after the target, determined by using SRIM.

Given a sample containing a mixture of N radioisotopes, the purity of the radionuclide of interest X is given by

$$P_X = \frac{A_X}{\sum_i^N A_i} \quad (3)$$

where A_X is the activity of the ith radionuclide.

2.4. ^{44}Sc production tests

The target used for the production tests was prepared by compressing approximately 66 mg of enriched $^{47}TiO_2$ powder, with the application of an axial force of about 4 $\cdot 10^4$ N. Being the diameter of the pellet 6 mm, the density of the pressed material was calculated by measuring the mass and thickness of the pellet and it was found to be (2.46 ± 0.07) g cm^{-3}.

The pellet was placed in a special capsule - called coin - realized by our group and successfully used to produce several radionuclides (Dellepiane et al., 2021). The coin is composed of two aluminum halves, the lid and the cup, kept together by small permanent magnets. The thickness of the lid is used to adjust the energy of the protons on the target material. The cup hosts the 6-mm-diameter pellet and an O-ring to prevent the leakage of possible molten material or of any gas produced during the irradiation.

The coin containing the enriched $^{47}TiO_2$ pellet was placed in an adapted target holder and positioned in the station used for cross-section measurements. In this configuration, high beam intensities cannot be achieved as the station is devoid of a cooling system. However, this irradiation method has the advantage of a precisely known beam current on the target, an essential feature for verifying consistency with cross-section measurements.

3. Experimental results

3.1. Cross-section measurements

In the investigated energy region, ^{44}Sc is produced directly from ^{47}Ti via the (p,α) reaction and indirectly via the ^{47}Ti(p,α)^{44m}Sc→^{44}Sc, which occurs both during the irradiation and after the EoB, during the cooling and measuring time. To determine the direct production cross section, short irradiation and cooling times were considered. In fact, considering short irradiation times and measuring the samples immediately after the end of beam, it was estimated that the ^{44m}Sc contamination was of the order of a few percent (<3%). The results are presented in Fig. 1; for completeness, the numerical values are reported in the Appendix (Table 5). Our measurements are in good agreement with the data reported in the literature (Levkowskij, 1991), while TENDL-2021 (Koning and Rochman, 2012) predictions overestimate the experimental results. In accordance with the findings of Takacs et al. (2002), the values presented in Ref. Levkowskij (1991) were scaled by a factor of 0.8, on the basis of the currently accepted value of the monitor reaction that was used by Levkovskij in his original work.

^{44m}Sc is the main impurity that would be produced by irradiating an enriched ^{47}Ti target. The cross section of the ^{47}Ti(p, α)^{44m}Sc nuclear reaction is shown in Fig. 2, together with the experimental data reported in the literature (Levkowskij, 1991). A good agreement was found over the whole energy range, while TENDL-2021 predictions seem to underestimate the experimental data at high energies. For completeness, the numerical values of the measured cross section are reported in the Appendix (Table 6).

^{43}Sc is produced from ^{46}Ti and ^{47}Ti via the (p,α) and (p,αn) nuclear reactions, respectively. The cross section of the first reaction was previously measured by our group as part of a project on the production of ^{43}Sc and is reported in Ref. Carzaniga et al. (2017). These data were used to correct the ^{43}Sc production cross section, in order to derive the contribution of the ^{47}Ti(p,αn)^{43}Sc nuclear reaction. The results of the production cross section and of the ^{47}Ti(p,αn) nuclear reaction cross section are shown in Fig. 3 and Fig. 4, respectively. For completeness, the numerical values are given in the Appendix (Table 7).

Two nuclear reactions produce ^{46}Sc in the energy range of interest, namely, ^{47}Ti(p,2p)^{46}Sc and ^{49}Ti(p,α)^{46}Sc. However, due to the low isotopic abundance of ^{49}Ti in the enriched $^{47}TiO_2$ powder, the second contribution was found to be negligible. During the irradiation, the ground state and a short-lived metastable state, denoted as ^{46m}Sc, are populated. ^{46m}Sc has a half-life of 18.75 s and completely decays into the ground state by an IT process; the ^{46}Sc measured cross section is therefore of a cumulative type. The results of the ^{47}Ti(p,2p)^{46}Sc reaction cross section are shown in Fig. 5; for completeness, the numerical values are reported in the Appendix (Table 8). Our measurements are in good agreement with the few data available in the literature

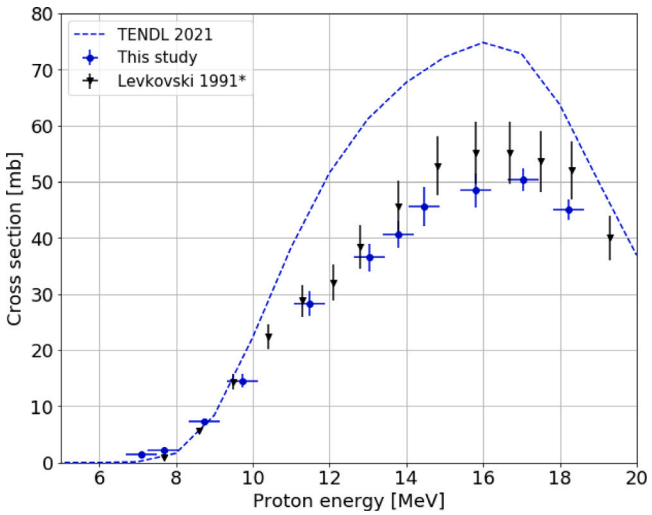

Fig. 1. ^{47}Ti(p,α)^{44}Sc cross section.

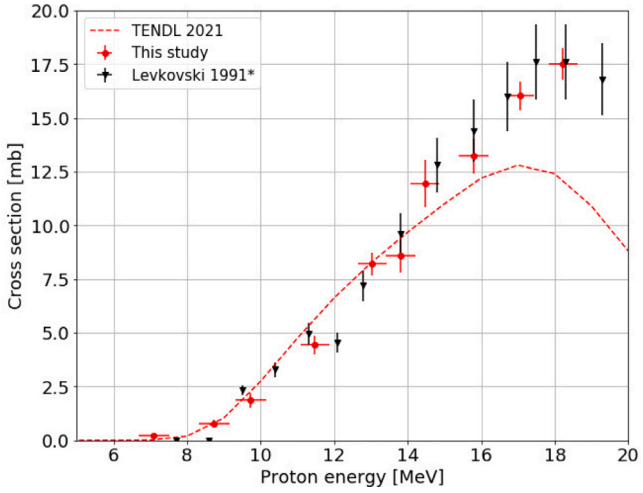

Fig. 2. ^{47}Ti(p,α)^{44m}Sc cross section.

in the energy range of interest (Levkowskij, 1991), but seem to be underestimated by TENDL-2021 predictions.

Furthermore, ^{47}Sc is produced from ^{48}Ti and ^{50}Ti via the (p,2p) and (p,α) nuclear reactions, respectively. The results of the ^{47}Sc production cross-section measurements are presented in Fig. 6 together with TENDL-2021 predictions.

A method based on the inversion of a linear system of equations (Braccini et al., 2022) was used to disentangle the contribution of the involved nuclear reactions to the production cross sections. This method requires measuring the total cross section with as many materials, with different isotopic compositions, as the number of the reactions involved in the production of the radionuclide being considered. For this purpose, the ^{47}Sc production cross section previously measured by our group (Dellepiane et al., 2022c) from 95.2% enriched $^{50}TiO_2$ (^{46}Ti: 0.01%; ^{47}Ti: 0.01%; ^{48}Ti: 0.23%; ^{49}Ti: 4.57%; ^{50}Ti: 95.2%) targets was considered. The ^{48}Ti(p,2p)^{47}Sc cross-section measurements calculated using this method are shown in Fig. 7, together with TENDL-2021 prediction and the experimental values available in the literature (Levkowskij, 1991). For completeness, the numerical values of the production cross section and of the ^{48}Ti(p,2p)^{47}Sc nuclear reaction cross section are reported in the Appendix (Table 9).

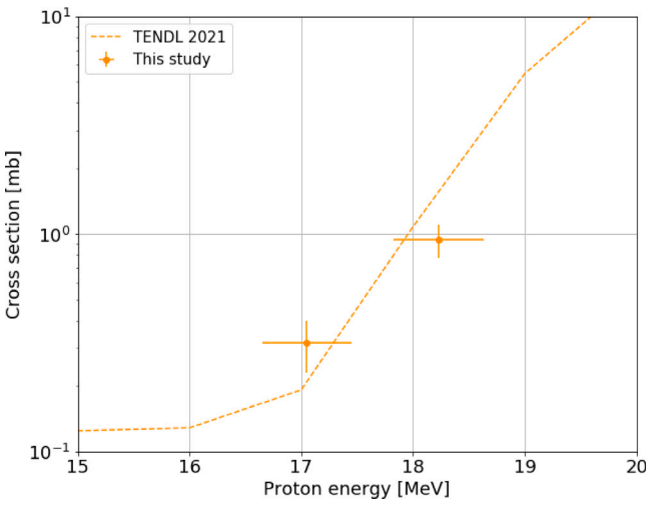

Fig. 3. ^{43}Sc production cross section from enriched $^{47}TiO_2$, whose isotopic composition is reported in Table 2. The nuclear reactions involved are ^{46}Ti(p,α)^{43}Sc and ^{47}Ti(p,αn)^{43}Sc.

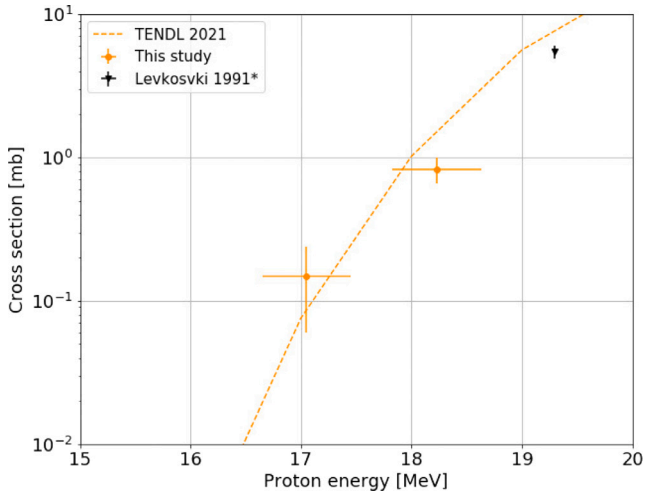

Fig. 4. ^{47}Ti(p,αn)^{43}Sc cross section.

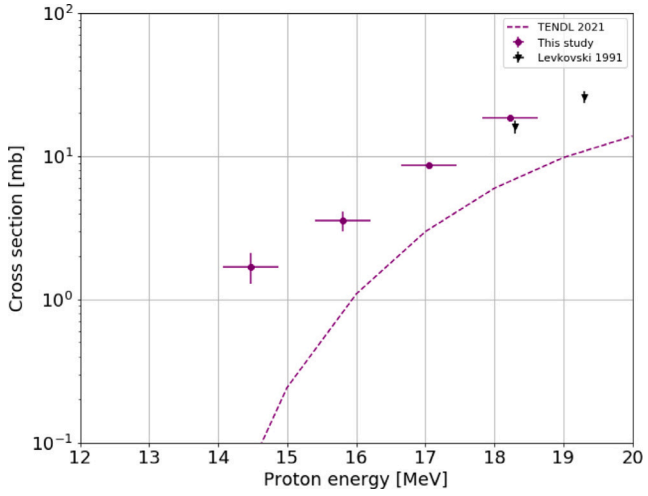

Fig. 5. ^{47}Ti(p,2p)^{46}Sc cross section.

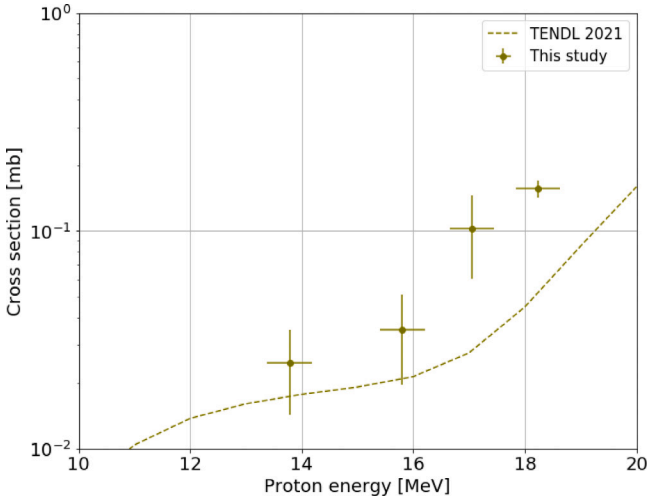

Fig. 6. ^{47}Sc production cross section from enriched $^{47}TiO_2$, whose isotopic composition is reported in Table 2. The nuclear reactions involved are ^{48}Ti(p,2p)^{47}Sc and ^{50}Ti(p,α)^{47}Sc.

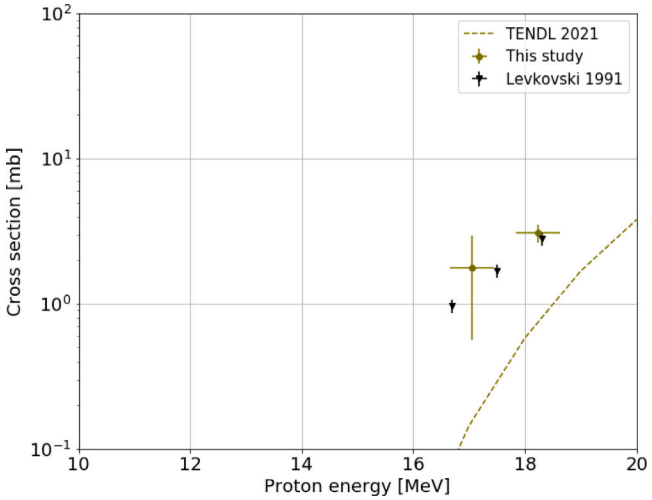

Fig. 7. ^{48}Ti(p,2p)^{47}Sc cross section.

3.2. ^{44}Sc production tests with solid targets

The irradiation of a 99.70% enriched $^{47}TiO_2$ target results in the production of several scandium radioisotopes. Among them, ^{44m}Sc, ^{46}Sc and ^{47}Sc have longer half-lives than ^{44}Sc and cannot be removed from the sample by means of the decay time.

The TTY of the Sc radioisotopes, calculated with Eq. (1) considering 1-h irradiation, is shown in Fig. 8 as a function of the entry energy. The production of ^{46}Sc and ^{47}Sc can be minimized by setting the beam input energy close or below the threshold energy of the ^{47}Ti(p,2p)^{46}Sc and ^{48}Ti(p,2p)^{47}Sc nuclear reactions (about 12 MeV and 13 MeV, respectively). The latter contribution can be further reduced by considering higher enriched materials.

The co-production of the relatively long-lived metastable state ^{44m}Sc cannot be avoided and it turns to be the main impurity. Its presence leads to the decrease in radionuclidic purity over time, limiting the application period of the labeled compound, and complicating the dosimetry of the patient.

^{43}Sc has a half-life comparable to ^{44}Sc and it is characterized by a high emission of low-energy positrons ($E_{\beta+}$ = 508 keV (70.9%); 634 keV (17.2%)) without any high-energy γ-ray. Therefore, it does not affect the image quality nor increases the dose to the patient. Despite these premises, further studies need to be carried out to assess the influence of ^{43}Sc on the ^{44}Sc-labeled radiotracer imaging performances. For this reason, ^{43}Sc is considered as an impurity in the calculations below. The ^{44}Sc TTY and the radionuclidic purity (Eq. (3)) are shown in Fig. 9 as a function of the proton entry energy. Considering an input energy of 15 MeV, which provides a good balance between the production yield and radionuclidic purity, a ^{44}Sc TTY of 48 MBq/μA with a purity of 98.2% can be achieved in 1-h irradiation. To obtain larger ^{44}Sc activities, longer irradiation times can be considered. In this case, however, the increased production of long-lived radionuclides, in particular ^{44m}Sc, must be taken into account.

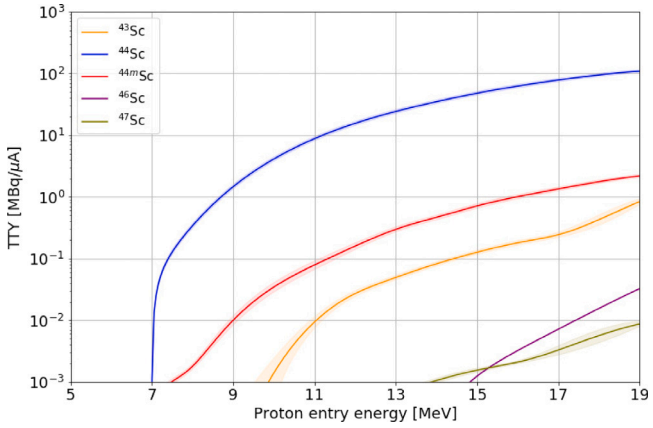

Fig. 8. TTY of Sc radioisotopes as a function of the proton entry energy for 1-h irradiation. The bands correspond to the maximum and minimum yield derived from the measured cross sections.

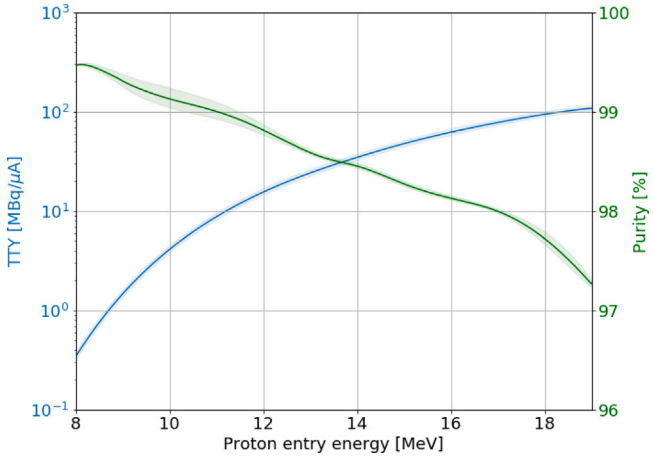

Fig. 9. ^{44}Sc TTY and radionuclidic purity as a function of the proton entry energy for 1-h irradiation. The bands correspond to the maximum and minimum yield derived from the measured cross sections.

To confirm these predictions based on cross-section measurements, two production tests were performed at 13.0 MeV and 15.0 MeV, by irradiating twice the 0.97-mm-thick enriched $^{47}TiO_2$ pellet. After the first irradiation, the pellet was measured with the HPGe detector and then let to decay for about 120 days in order to be reused.

The incident energies, the irradiation parameters and the activities obtained in the two tests are reported in Table 4. The experimental results, together with the production yields and the radionuclidic purity calculated in our irradiation condition on the basis of the cross sections we measured, are shown in Fig. 10 as a function of the proton entry energy. It is important to remark that all irradiation times were much shorter than the half-lives of the involved radioisotopes, and therefore

Table 4
Irradiation parameters (input and output beam energy, integrated current and irradiation time), radioisotope activities and ^{44}Sc purity obtained irradiating the 0.97-mm-thick enriched $^{47}TiO_2$ pellet in the BTL. The values in brackets are the yield calculations based on the cross section measurements.

	Irradiation 1	Irradiation 2
E_{in} [MeV]	13.0 ± 0.4	15.0 ± 0.4
E_{out} [MeV]	3.9 ± 0.4	7.7 ± 0.4
Q [E-3 μAh]	0.87 ± 0.04	0.63 ± 0.03
t_i [s]	520 ± 1	809 ± 1
Production Yield [MBq/μAh]		
^{43}Sc	No Signal *(0.05)*	0.11 ± 0.04 *(0.13)*
^{44}Sc	28 ± 2 *(25)*	48 ± 3 *(48)*
^{44m}Sc	0.28 ± 0.02 *(0.29)*	0.73 ± 0.04 *(0.72)*
^{46}Sc	No Signal *(0.07E−3)*	(0.9 ± 0.1)E-3 *(1.2E−3)*
^{47}Sc	(1.0 ± 0.1)E-3 *(0.7E−3)*	(1.9 ± 0.8)E-3 *(1.5E−3)*
Purity [%]	99.01 ± 0.09 *(98.58)*	98.28 ± 0.16 *(98.27)*

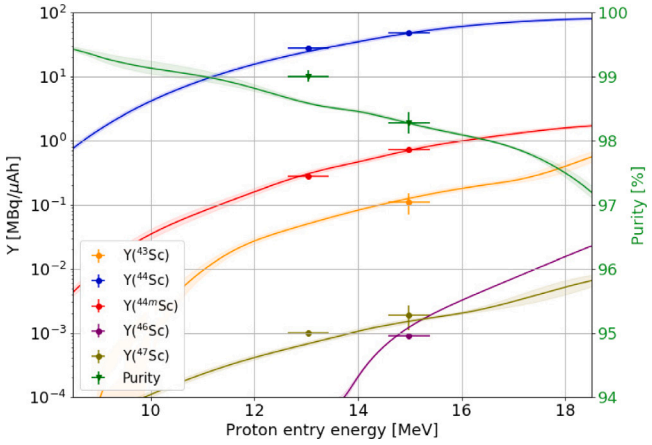

Fig. 10. Production yields of Sc radioisotopes and radionuclidic purity as a function of the proton entry energy. The dots are the experimental points, the lines are calculations based on the cross sections measured.

Eq. (1) can be approximated linearly with respect to time ($\lambda t_i \ll 1$). In this approximation, the production yield can be given in MBq/μAh.

In the first production, ^{43}Sc could not be measured with the HPGe detector due to the low activity produced and its half-life comparable with the one of ^{44}Sc. For this reason, the experimental purity was slightly overestimated. In the other cases, a good agreement was found.

4. Conclusion and outlook

Scandium radionuclides are among the most promising for theranostic applications in nuclear medicine and their optimized production using solid targets is currently being studied at the Bern medical cyclotron laboratory, where an 18 MeV IBA HC cyclotron is in operation. Among the several routes investigated, the use of enriched ^{46}Ti, ^{47}Ti, and ^{50}Ti targets would enable the production of ^{43}Sc, ^{44}Sc, and ^{47}Sc, respectively, using a single medical cyclotron facility. Furthermore, it would allow to employ the same radiochemical separation and labeling procedures.

The aim of this study was therefore to investigate the feasibility of ^{44}Sc production by proton irradiation of enriched ^{47}Ti, exploiting the ^{47}Ti(p,α)^{44}Sc nuclear reaction. To select the optimal irradiation conditions, the cross section of the nuclear reactions involved in the production of Sc radioisotopes were measured in the energy range of interest, by irradiating 95.7% enriched $^{47}TiO_2$ targets.

According to our findings, considering the optimal input energy of 15 MeV, a ^{44}Sc TTY of 48 MBq/μA with a radionuclidic purity of 98.2% can be achieved in 1-h irradiation. The main impurities were found to be ^{44m}Sc (about 1.5%) and ^{43}Sc (about 0.3%). Based on the isotopic composition of the material used, traces of ^{46}Sc and ^{47}Sc can also be produced (<0.006% in the case of the material used in this study). It is important to remark that the presence of ^{43}Sc in the final product may not be a problem or could even be beneficial. In fact, ^{43}Sc is a β^+-emitter under investigation for PET diagnostics, with a half-life comparable to ^{44}Sc. Therefore, it does not degrade the image quality and, having no high-energy γ emissions, it does not lead to an increase of the dose absorbed by the patient and by the personnel.

The results obtained were confirmed by successfully performing ^{44}Sc production tests in the energy range of interest. A 66-mg 95.7% enriched $^{47}TiO_2$ pellet was used for this purpose.

The ^{47}Ti(p,α)^{44}Sc reaction shows a lower production yield compared to the ^{44}Ca(p,n)^{44}Sc (about 48 MBq/μA vs 520 MBq/μA for 1-h irradiation). However, the higher isotopic abundance of ^{47}Ti compared to ^{44}Ca (7.4% vs 2.1%) and the easier handling of the target could make this production route a promising alternative. Furthermore, according to the findings of Loveless et al. (2021), TiO_2 targets can tolerate very high beam currents, easily reachable with modern medical cyclotrons, allowing to achieve higher activities.

The results obtained in this study, along with our previous works (Carzaniga et al., 2017; Dellepiane et al., 2022c), represent a step towards the production of Sc radioisotopes for theranostic applications in nuclear medicine at a single medical cyclotron facility.

CRediT authorship contribution statement

Gaia Dellepiane: Writing – review & editing, Writing – original draft, Validation, Software, Methodology, Investigation, Formal analysis, Data curation, Conceptualization. **Pierluigi Casolaro:** Writing – review & editing, Investigation, Conceptualization. **Alexander Gottstein:** Investigation. **Isidre Mateu:** Methodology, Investigation. **Paola Scampoli:** Writing – review & editing, Investigation, Conceptualization. **Saverio Braccini:** Writing – review & editing, Supervision, Resources, Project administration, Methodology, Investigation, Funding acquisition, Conceptualization.

Declaration of competing interest

The authors declare that they have no known competing financial interests or personal relationships that could have appeared to influence the work reported in this paper.

Data availability

Data will be made available on request.

Acknowledgments

We acknowledge contributions from LHEP engineering and technical staff (Roger Hänni and Jan Christen, in particular) and from the SWAN Isotopen AG team (Riccardo Bosi and Michel Eggemann, in particular). This research project was partially funded by the Swiss National Science Foundation (SNSF) (grants: CRSII5_180352, 200021_175749 and 200021_188495).

Appendix

See Tables 5–9.

Table 5
Cross-section data of the $^{47}Ti(p,\alpha)^{44}Sc$ nuclear reaction.

E [MeV]	$^{47}Ti(p,\alpha)^{44}Sc$ [mbarn]
7.1 ± 0.4	1.4 ± 0.2
7.7 ± 0.4	2.2 ± 0.2
8.7 ± 0.4	7.2 ± 0.6
9.7 ± 0.4	15 ± 1
11.5 ± 0.4	28 ± 2
13.0 ± 0.4	37 ± 3
13.8 ± 0.4	41 ± 2
14.5 ± 0.4	46 ± 4
15.8 ± 0.4	48 ± 3
17.1 ± 0.4	50 ± 2
18.2 ± 0.4	45 ± 2

Table 6
Cross-section data of the $^{47}Ti(p,\alpha)^{44m}Sc$ nuclear reaction.

E [MeV]	$^{47}Ti(p,\alpha)^{44m}Sc$ [mbarn]
7.1 ± 0.4	0.23 ± 0.03
7.7 ± 0.4	–
8.7 ± 0.4	0.8 ± 0.2
9.7 ± 0.4	1.9 ± 0.3
11.5 ± 0.4	4.4 ± 0.4
13.0 ± 0.4	8.2 ± 0.5
13.8 ± 0.4	8.6 ± 0.8
14.5 ± 0.4	12.0 ± 1.1
15.8 ± 0.4	13.2 ± 0.8
17.1 ± 0.4	16.0 ± 0.7
18.2 ± 0.4	17.5 ± 0.7

Table 7
^{43}Sc production cross section and $^{47}Ti(p,\alpha n)^{43}Sc$ cross-section data.

E [MeV]	$^{enr-47}Ti(p,X)^{43}Sc$ [mbarn]	$^{47}Ti(p,\alpha n)^{43}Sc$ [mbarn]
15.8 ± 0.4	No Signal	No Signal
17.1 ± 0.4	0.32 ± 0.08	0.15 ± 0.09
18.2 ± 0.4	0.9 ± 0.2	0.8 ± 0.2

Table 8
Cross-section data of the $^{47}Ti(p,2p)^{46}Sc$ nuclear reaction.

E [MeV]	$^{47}Ti(p,2p)^{46}Sc$ [mbarn]
13.8 ± 0.4	No Signal
14.5 ± 0.4	1.7 ± 0.4
15.8 ± 0.4	3.6 ± 0.6
17.1 ± 0.4	8.6 ± 0.5
18.2 ± 0.4	18.5 ± 1.0

Table 9
^{47}Sc production cross section and $^{48}Ti(p,2p)^{47}Sc$ cross-section data.

E [MeV]	$^{enr-47}Ti(p,X)^{47}Sc$ [mbarn]	$^{48}Ti(p,2p)^{47}Sc$ [mbarn]
14.5 ± 0.4	0.031 ± 0.002	No Signal
15.8 ± 0.4	0.036 ± 0.002	No Signal
17.1 ± 0.4	0.10 ± 0.04	1.8 ± 1.2
18.2 ± 0.4	0.16 ± 0.01	3.1 ± 0.4

References

Auger, M., Braccini, S., Carzaniga, T.S., Ereditato, A., Nesteruk, K.P., Scampoli, P., 2016. A detector based on silica fibers for ion beam monitoring in a wide current range. J. Instrum. 11 (03), P03027. http://dx.doi.org/10.1088/1748-0221/11/03/p03027.

Auger, M., Braccini, S., Ereditato, A., Nesteruk, K.P., Scampoli, P., 2015. Low current performance of the Bern medical cyclotron down to the pA range. Meas. Sci. Technol. 26, http://dx.doi.org/10.1088/0957-0233/26/9/094006.

Braccini, S., 2013. The new Bern PET cyclotron, its research beam line, and the development of an innovative beam monitor detector. AIP Conf. Proc. 1525, 144–150. http://dx.doi.org/10.1063/1.4802308.

Braccini, S., 2017. Compact medical cyclotrons and their use for radioisotope production and multidisciplinary research. Proceed. Cyclotrons2016 TUD01, 229–234.

Braccini, S., Carzaniga, T.S., Dellepiane, G., Grundler, P.V., Scampoli, P., van der Meulen, N.P., Wüthrich, D., 2022. Optimization of ^{68}Ga production at an 18 MeV medical cyclotron with solid targets by means of cross-section measurement of ^{66}Ga, ^{67}Ga and ^{68}Ga. Appl. Radiat. Isot. 110252. http://dx.doi.org/10.1016/j.apradiso.2022.110252.

Braccini, S., Scampoli, P., 2016. Science with a medical cyclotron. CERN Courier 21–22.

Carzaniga, T.S., Auger, M., Braccini, S., Bunka, M., Ereditato, A., Nesteruk, K.P., Scampoli, P., Türler, A., van der Meulen, N.P., 2017. Measurement of ^{43}Sc and ^{44}Sc production cross-section with an 18 MeV medical PET cyclotron. Appl. Radiat. Isot. 129, 96–102. http://dx.doi.org/10.1016/j.apradiso.2017.08.013.

CIAAW, 2023. Isotopic composition of the elements. URL https://www.ciaaw.org/isotopic-abundances.htm. (Last Access 10 January 2023).

Dellepiane, G., Aguilar, C.B., Carzaniga, T.S., Casolaro, P., Häffner, P., Scampoli, P., Schmid, M., Braccini, S., 2021. Research on theranostic radioisotope production at the Bern medical cyclotron. IL Nuovo Cimento C 44, http://dx.doi.org/10.1393/ncc/i2021-21130-6.

Dellepiane, G., Casolaro, P., Favaretto, C., Grundler, P.V., Mateu, I., Scampoli, P., Talip, Z., van der Meulen, N.P., Braccini, S., 2022a. Cross section measurement of terbium radioisotopes for an optimized ^{155}Tb production with an 18 MeV medical PET cyclotron. Appl. Radiat. Isot. 184, 110175. http://dx.doi.org/10.1016/j.apradiso.2022.110175.

Dellepiane, G., Casolaro, P., Gottstein, A., Mateu, I., Scampoli, P., Braccini, S., 2023. Optimized production of ^{67}Cu based on cross section measurements of ^{67}Cu and ^{64}Cu using an 18 MeV medical cyclotron. Appl. Radiat. Isot. 195, 110737. http://dx.doi.org/10.1016/j.apradiso.2023.110737.

Dellepiane, G., Casolaro, P., Mateu, I., Scampoli, P., Braccini, S., 2022b. Alternative routes for ^{64}Cu production using an 18 MeV medical cyclotron in view of theranostic applications. Appl. Radiat. Isot. 110518. http://dx.doi.org/10.1016/j.apradiso.2022.110518.

Dellepiane, G., Casolaro, P., Mateu, I., Scampoli, P., Voeten, N., Braccini, S., 2022c. ^{47}Sc and ^{46}Sc cross-section measurement for an optimized ^{47}Sc production with an 18 MeV medical PET cyclotron. Appl. Radiat. Isot. 189, 110428. http://dx.doi.org/10.1016/j.apradiso.2022.110428.

Dellepiane, G., Casolaro, P., Mateu, I., Scampoli, P., Voeten, N., Braccini, S., 2022d. Cross-section measurement for an optimized ^{61}Cu production at an 18 MeV medical cyclotron from natural Zn and enriched ^{64}Zn solid targets. Appl. Radiat. Isot. 190, 110466. http://dx.doi.org/10.1016/j.apradiso.2022.110466.

Durán, M.T., Juget, F., Nedjadi, Y., Bailat, C., Grundler, P.V., Talip, Z., van der Meulen, N.P., Casolaro, P., Dellepiane, G., Braccini, S., 2022. Half-life measurement of ^{44}Sc and ^{44m}Sc. Appl. Radiat. Isot. 190, 110507. http://dx.doi.org/10.1016/j.apradiso.2022.110507.

Forgács, A., Balkay, L., Trón, L., Raics, P., 2014. Excel2Genie: A microsoft excel application to improve the flexibility of the genie-2000 spectroscopic software. Appl. Radiat. Isot. 94, 77–81. http://dx.doi.org/10.1016/j.apradiso.2014.07.005.

Häffner, P.D., Aguilar, C.B., Braccini, S., Scampoli, P., Thonet, P.A., 2019. Study of the extracted beam energy as a function of operational parameters of a medical cyclotron. Instruments 3 (63), http://dx.doi.org/10.3390/instruments3040063.

IAEA, 2022. Live chart of nuclides, available online. URL https://nds.iaea.org/relnsd/vcharthtml/VChartHTML.html. (Last Access 08 April 2022).

International Standard, 2021. Nuclear Instrumentation – Measurement of Activity Or Emission Rate of Gamma-Ray Emitting Radionuclides – Calibration and Use of Germanium-Based Spectrometers. IEC 61452:2021.

Isoflex, 2022. Isotope for science, medicine and industry. URL http://www.isoflex.com/. (Last Access 14 October 2022).

Juget, F., Durán, M.T., Nedjadi, Y., Talip, Z., Grundler, P.V., Favaretto, C., Casolaro, P., Dellepiane, G., Braccini, S., Bailat, C., van der Meulen, N.P., 2023. Activity measurement of ^{44}Sc and calibration of activity measurement instruments on production sites and clinics. Molecules 28, 1345. http://dx.doi.org/10.3390/molecules28031345.

Koning, A., Rochman, D., 2012. Modern Nuclear Data Evaluation With The TALYS Code System. Nucl. Data Sheets 113, 2841–2934. http://dx.doi.org/10.1016/j.nds.2012.11.002.

Krajewski, S., Cydzik, I., Abbas, K., Bulgheroni, A., Simonelli, F., Holzwarth, U., Bilewicz, A., 2013. Cyclotron production of ^{44}Sc for clinical application. Radiochim. Acta 101 (5), 333–338. http://dx.doi.org/10.1524/ract.2013.2032.

Levkowskij, V.N., 1991. Activation Cross Sections for the Nuclides of Medium Mass Region (A=40-100) with Protons and α-particles at Medium (E=10-50 MeV) energies. Inter-Vesti, Moscow.

Loveless, C.S., Blanco, J.R., Diehl, G.L., Elbahrawi, R.T., Carzaniga, T.S., Braccini, S., Lapi, S.E., 2021. Cyclotron production and separation of scandium radionuclides from natural titanium metal and titanium dioxide targets. J. Nucl. Med. 62 (1), 131–136. http://dx.doi.org/10.2967/jnumed.120.242941.

Mirion Technologies, 2022. GENIE 2000 - basic spectroscopy software. URL https://www.mirion.com/products/genie-2000-basic-spectroscopy-software. (Last Access 12 October 2022).

Müller, C., Bunka, M., Reber, J., Fischer, C., Zhernosekov, K., Türler, A., Schibli, R., 2013. Promises of cyclotron-produced ^{44}Sc as a diagnostic match for trivalent β^--emitters: In vitro and in vivo study of a ^{44}Sc-DOTA-folate conjugate. J. Nuclear Medicine 54 (12), 2168–2174. http://dx.doi.org/10.2967/jnumed.113.123810.

Nesteruk, K.P., Auger, M., Braccini, S., Carzaniga, T.S., Ereditato, A., Scampoli, P., 2018. A system for online beam emittance measurements and proton beam characterization. J. Instrum. 13, P01011. http://dx.doi.org/10.1088/1748-0221/13/01/p01011.

Potkins, D.E., Braccini, S., Nesteruk, K.P., Carzaniga, T.S., Vedda, A., Chiodini, N., Timmermans, J., Melanson, S., Dehnel, M.P., 2017. A low-cost beam profiler based on cerium-doped silica fibers. In: Proceedings of CAARI-16, Physics Procedia. http://dx.doi.org/10.1016/j.phpro.2017.09.061.

Radchenko, V., Meyer, C.A.L., Engle, J., Naranjo, C., Unc, G., Mastren, T., Brugh, M., Birnbaum, E., John, K., Nortier, F., Fassbender, M., 2016. Separation of ^{44}Ti from proton irradiated scandium by using solid-phase extraction chromatography and design of ^{44}Ti/^{44}Sc generator system. J. Chromatogr. A 1477, 39–46. http://dx.doi.org/10.1016/j.chroma.2016.11.047.

Roesch, F., 2012. Scandium-44: Nenefits of a long-lived PET radionuclide available from the ^{44}Ti/^{44}Sc generator system. Curr. Radiopharmaceut. 5 (3), 187–201. http://dx.doi.org/10.2174/1874471011205030187.

Sandia National Laboratories, 2022. InterSpec - spectral radiation analysis software. URL https://sandialabs.github.io/InterSpec/. (Last Access 12 October 2022).

Sitarz, M., Szkliniarz, K., Jastrzębski, J., Choiński, J., Guertin, A., Haddad, F., Jakubowski, A., 2018. Production of Sc medical radioisotopes with proton and deuteron beams. Appl. Radiat. Isot. 142, 104–112. http://dx.doi.org/10.1016/j.apradiso.2018.09.025.

Szkliniarz, K., Sitarz, M., Walczak, R., Jastrzębski, J., Bilewicz, A., Choiński, J., Jakubowski, A., Majkowska, A., Stolarz, A., Trzcińska, A., Zipper, W., 2016. Production of medical Sc radioisotopes with an alpha particle beam. Appl. Radiat. Isot. 118, 182–189. http://dx.doi.org/10.1016/j.apradiso.2016.07.001.

Takacs, S., Tarkanyi, F., Sonck, M., Hermanne, A., 2002. Investigation of the ^{nat}Mo(p,x)^{96mg}Tc nuclear reaction to monitor proton beams: New measurements and consequences on the earlier reported data. Nucl. Instrum. Methods Phys. Res. B 198, 183–196.

van der Meulen, N.P., Bunka, M., Domnanich, K.A., Müller, C., Haller, S., Vermeulen, C., Türler, A., Schibli, R., 2015. Cyclotron production of ^{44}Sc: From bench to bedside. Nucl. Med. Biol. 42 (9), 745–751. http://dx.doi.org/10.1016/j.nucmedbio.2015.05.005.

van der Meulen, N.P., Hasler, R., Talip, Z., Grundler, P.V., Favaretto, C., Umbricht, C.A., Müller, C., Dellepiane, G., Carzaniga, T.S., Braccini, S., 2020. Developments toward the implementation of ^{44}Sc production at a medical cyclotron. Molecules 25, 1–16. http://dx.doi.org/10.3390/molecules25204706.

Ziegler, J.F., Manoyan, J.M., 2013. The stopping of ions in compounds. Nucl. Instrum. Methods B 35, 215, URL http://www.srim.org.